

## Reply to Referee #1

We would like to thank Referee #1 for the time spent to read our manuscript and for the positive comment concerning the application of a comprehensive photochemical modelling system coupled with a Fugacity Level-III multi-media model. We will consider the comments in the revision of the manuscript, as it is stated below.

- 1. The authors have used the EMEP model for the chemical transport simulations of a hypothetical CCP point source. Point source in-plume concentrations are sensitive to plume rise, chemistry, vertical diffusion and horizontal diffusion and thus all of these processes need to be considered for this source geometry. However, the state equation in Simpson (2012) does not include a horizontal diffusion term (as acknowledged in the Simpson paper). While it is acknowledged that horizontal diffusion in grid models can be dominated by numerical diffusion due to the finite differencing approaches used in advection schemes (and the treatment of the point source as a volume source), horizontal diffusion under convective conditions can dominate numerical diffusion, particularly for the small grid horizontal grid spacing used in this study.***

### Response:

The physical processes to be modelled as diffusion in chemical transport models are different in different scales. By definition, diffusion processes are sub-grid mixing processes not resolved by the given resolution of the model. Therefore, the horizontal diffusion coefficient, which is a measure of the strength of the atmospheric turbulence, will depend on the grid resolution. For large grid cells (50x50 km<sup>2</sup> or 150x150 km<sup>2</sup>) the numerical diffusion will usually be much larger than the physical diffusion at these scales. Therefore no additional diffusion term has been included in the EMEP model when using a 50-km grid resolution (see Simpson et al., 2012). At higher resolution scales, however, the physical diffusion will gradually become more important than numerical diffusion, and becomes greater than numerical diffusion for 5x5 km<sup>2</sup> cells or below.

The referee has a point that neglecting the horizontal diffusion operator is especially problematic under unstable (convective) conditions. The distance between the midpoints of two neighboring cells in the inner nest is 2000 m. Horizontal dispersion sigma parameters calculated according to Pasquill-Gifford show that sigma in horizontal direction is about 400 m for a 2-km resolution grid (one-sided diffusion) for unstable conditions. The sigma values are much lower (about 100 m) for neutral or more stable conditions. Thus the error introduced by neglecting horizontal diffusion under convective conditions at this scale could be up to 400/2000, corresponding to 20%. Taking into account horizontal diffusion is expected to result in a wider plume and a decrease of the maximum ground-level concentration in the plume centerline.

In order to estimate the error related to neglecting horizontal diffusion in the inner domain for WRF-EMEP simulations, we performed a test for dispersion in horizontal direction with the Eulerian model EPISODE (Walker et al., 1999; Slørdal et al., 2003). In both EMEP and EPISODE, the numerical solution of the advection terms is based upon the scheme of Bott; the fourth order scheme is utilized in the horizontal directions. The Bott scheme intends to reduce the numerical diffusion. However even at fine scales there might still be some numerical diffusion, depending on how well the plume is delimited in space and on the wind fields (Courant

number). In the applied version of EPISODE all operators can be turned on or off for testing purposes.

The test was done for the horizontal dispersion from a 2000 m wide volume source (emission of an inert tracer with 1 g/s) on a 2-km resolution grid with layer height of 90 m. We used unstable conditions (ambient temperature gradient  $dT/dz = -0.02$  K/m), a mixing layer height of 1000 m, and a constant horizontal wind from 45 degrees with wind speed  $u = 3$  m/s. The first run considered only transport by horizontal advection while the second run considered both horizontal advection and diffusion (see Figure C1). Only in a distance of more than 20 km downwind from the source, significant differences of the horizontal dispersion of the plume became apparent. In 9 km distance, the ground-level concentration was reduced by 12% in the plume centerline and by 2-6% in the adjacent cells, when including horizontal diffusion. In 20 km distance, the ground-level concentration was reduced by 20% in the plume centerline and by 10-12% in the adjacent cells, when including horizontal diffusion.

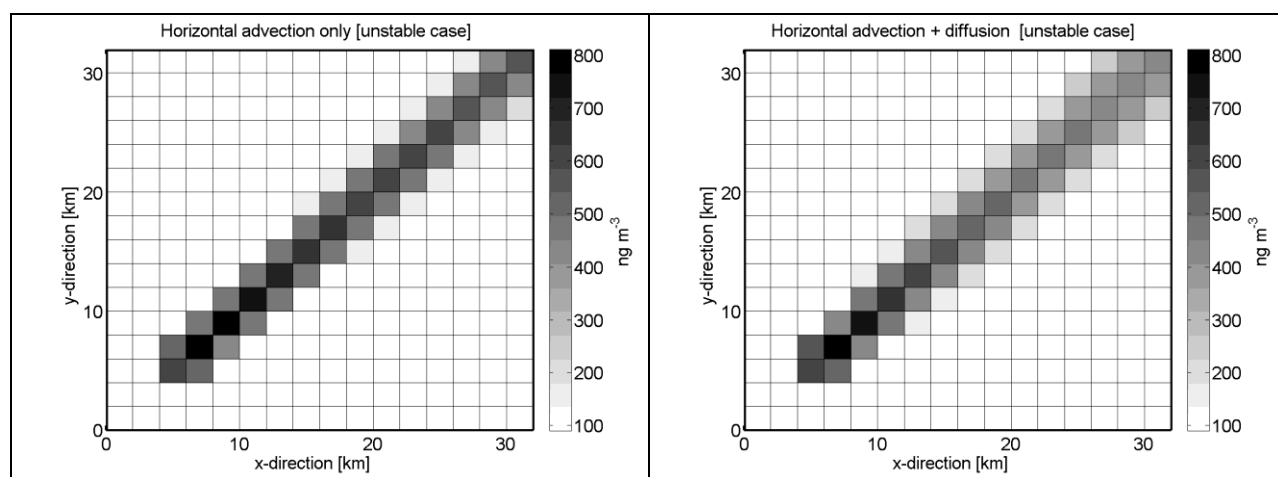


Figure C1: Horizontal dispersion test with EPISODE on 2-km scale for unstable conditions: a) ground-level concentrations (in  $\text{ng m}^{-3}$ ) when only horizontal advection is operative, and b) ground-level concentrations when horizontal advection and horizontal diffusion are operative. Volume source ( $2000 \times 2000 \times 90 \text{ m}^3$ ) with emission of  $1 \text{ g s}^{-1}$  was placed in the grid cell at  $x = 5$  km,  $y = 5$  km. In the test, the ambient temperature gradient was  $dT/dz = -0.02 \text{ K m}^{-1}$ , mixing layer height was 1000 m, and horizontal wind from 45 degrees was constant with wind speed  $u = 3 \text{ m s}^{-1}$ .

In WRF-EMEP simulations, maximum ground-level concentrations of amines were always found within a radius of 10 km distance from the source (Mongstad CCP). We therefore conclude that our modelled maximum amine concentrations are at most 15% higher than they would be with physical diffusion included.

Finally, we note that for our application of the WRF-EMEP model framework there are a number of other processes and terms (not at least chemistry) that introduce larger uncertainties and errors than horizontal atmospheric diffusion.

We will add a new section in the Supplement with heading “S3. Evaluation of horizontal dispersion in the EMEP model” to include the above discussion and Figure C1. Consequently, current section S3 (“Comparison of WRF meteorology to met station data”) becomes section S4.

The following note was added in section 2.2 (“Description of WRF-EMEP model system”), on page 8642, line 18:

“By definition, atmospheric transport by diffusion processes are sub-grid mixing processes not resolved by the given resolution of the model. For large grid cells (e.g.  $50 \times 50 \text{ km}^2$  as in the EMEP standard setup) the numerical diffusion will usually be much larger than the physical diffusion in horizontal direction. Therefore no additional horizontal diffusion term has been included in the EMEP model when using a 50-km grid resolution (see Simpson et al., 2012). However, at higher resolution scales, the physical diffusion will gradually become more important than numerical diffusion, and becomes greater than numerical diffusion for  $5 \times 5 \text{ km}^2$  cells or below. We estimate that the error related to neglecting horizontal diffusion in the inner domain ( $2 \times 2 \text{ km}^2$  cell size) is less than 15% for the modelled maximum amine ground-level concentrations (details can be found in section S3 of the Supplement).”

- 2. The sensitivity of ground-level concentrations to plume rise are likely to be partially an artefact of the coarse model spacing in the vertical. This is noted by the authors who comment that a refinement of the vertical structure of the EMEP is currently underway. In lieu of providing the results of additional simulations with a finer vertical structure for the paper it is suggested that the authors also highlight the impact of the relatively coarse vertical resolution in Section 3.4 where plume rise sensitivity is discussed. Another alternative is to use Gaussian plume modelling to investigate the sensitivity of near-source concentrations to the choice of plume rise algorithm.***

**Response:**

We agree with the referee that the current treatment of plume rise from elevated point sources may lead to inaccurate attribution of emitted material to vertical model layers due to the relatively coarse vertical resolution of the EMEP model. We have tested the sensitivity of the ground-level maximum concentration within 8 km downwind of the source by implementing the plume rise schemes of our work (“NILU Plume”, “PVDI Plume”, and “ASME Plume”) in a Gaussian plume model. The assumption in the Gaussian plume model included: flat terrain (appropriate for Mongstad within a radius of 8 km), mixing height of 1000 m, no effect of buildings (as in the EMEP model), and no stack downwash. Tests were done for three typical situations in the atmospheric boundary layer: neutral case with wind speed  $u = 5 \text{ m/s}$ , light stable case with  $u = 3 \text{ m/s}$ , and unstable case with  $u = 2 \text{ m/s}$  (see Figure C2).

For neutral conditions the result was a wide area with ground-level concentrations between 100 and  $400 \text{ ng m}^{-3}$  (1000 - 4500 m downwind the source). Effective emission height for “NILU Plume”, “PVDI Plume”, and “ASME Plume” was 139 m, 169 m, and 177 m, respectively. Since maximum ground level concentration ( $C_{\text{max}}$ ) is roughly proportional to the square of the effective emission height, the increase from 140 m to 180 m implies a potential decreasing  $C_{\text{max}}$  by 40%. This corresponds well with the result for the neutral case:  $C_{\text{max}}$  for “NILU Plume” is roughly twice as high as for the other two plume rise schemes. For “PVDI” and “ASME”, the location of  $C_{\text{max}}$  is shifted by about 1000 m in downwind direction compared to “NILU Plume”.

For light stable conditions,  $C_{\text{max}}$  is found in the largest distance from the source. Effective emission height for “NILU Plume”, “PVDI Plume”, and “ASME Plume” was 141 m, 242 m, and 162 m, respectively. The parameterization of “PVDI Plume” has been derived for neutral

conditions and does not consider atmospheric stability. The application of “PVDI Plume” in light stable conditions resulted in very low  $C_{max}$ , which occurs in 5500 m distance from the source. For the other two plume rise schemes, high ground-level concentrations are located between 2000 and 5000 m downwind from the source.

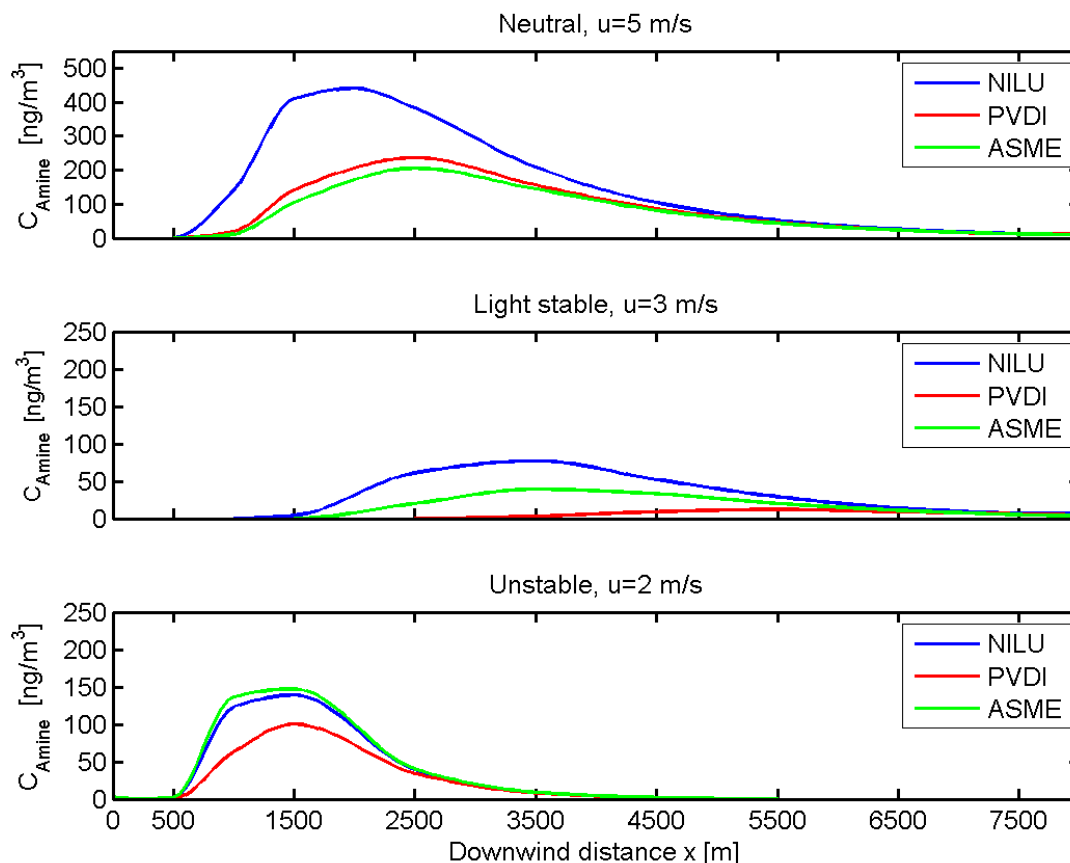


Figure C2: Sensitivity test of plume-rise parameterization with a Gaussian plume model, showing ground-level concentrations in the centerline of the plume as a function of the downwind distance from the elevated point source. Three typical situations in the atmospheric boundary layer are considered: neutral case with wind speed  $u = 5$  m/s (top), light stable case with  $u = 3$  m/s (middle), and unstable case with  $u = 2$  m/s (bottom).

For unstable conditions, all schemes give effective emission heights (range: 290-330 m).  $C_{max}$  is located in ca. 1500 m distance from the source, which would explain the high near-source concentrations of amines found in the EMEP simulations.

The test with the Gaussian plume model confirms the high sensitivity of the maximum ground level concentration to the respective parameterization of plume rise, especially under neutral and moderately stable conditions.

The discussion and Figure C2 will be added to section S2 (“Plume rise treatment in the EMEP model”) in the Supplement.

We added the following note in section 3.4 (“Results of the simulations”), on page 8655, line 11: “Tests with a simple Gaussian plume model confirmed the high sensitivity of the ground level concentrations of amines to the respective parameterization of plume rise, especially under neutral and moderately stable conditions (see section S2, and Figure S2).”

**3. Further to the plume rise discussion, the authors use equation (1) to estimate the wind speed at stack/plume height give the wind speed at the first model level. The use of (1) should be restricted to  $-Z/L < 0(2)$  for unstable conditions and  $Z/L > 1$  for stable conditions. Can the authors confirm that (1) is restricted only to applicable limits?**

**Response:**

Firstly, we excuse a typo in the display of Equation (1) in the manuscript: the Monin-Obukhov similarity function needs to be multiplied by  $1/v$  inside the integral,

$$u_z = u_{z_{ref}} + \frac{u_*}{K} \int_{v=z_{ref}}^{v=z} \frac{1}{v} \cdot \varphi_m(v, L^{-1}) dv \quad (1)$$

this had been correctly implemented in the code.

Secondly, in using Eq. (1) to estimate the wind speed at stack/plume height we currently do not restrict  $z/L$  to lie in the interval  $[-2, 0]$  for the unstable cases ( $L < 0$ ), and  $[0, 1]$  for the stable cases ( $L > 0$ ).

For the unstable cases, a re-calculation of the wind speed profiles using the limitation  $-2 \leq z/L < 0$  based on the meteorological data at the Mongstad site in July 2007 shows a maximum difference in wind speed at the final plume height of 0.36 m/s. This have thus had a negligible effect on the calculated final plume heights in these cases.

For the stable cases, we use the Högström (1996) formulation  $\varphi_m = 1 + 5.3 \cdot z/L$  for  $z/L \leq 1$ , but actually then use the formulation  $\varphi_m = 5.3 + z/L$  from Holtslag et al. (1990) for  $z/L > 1$ . Unfortunately, we left this last part of the formulation out in the description in the paper.

Using the limitation  $0 < z/L \leq 1$  for the stable cases results in a maximum deviation of the wind speed at the final plume height of 2.0 m/s at Mongstad in July 2007. The maximum deviation of the final plume height is 20 m for the stable conditions.

The impact of the deviation on the results computed with the WRF-EMEP model are however negligible since the occurrence of  $z/L > 1$  for stable conditions was limited to less than 1 % of the time in 2007 based on 3-hourly WRF meteorology.

For the future use of the wind profile function in our model code, we agree with the referee that it would be good to limit  $z/L$  to the above intervals. We will take steps to modify our code in accordance with this.

Equation (1) was corrected in the manuscript and a brief discussion on the limitations of Eq. (1) was added to section 2.4 (“Point source emissions”).

- 4. In section 2.2 the authors discuss the emissions of SO<sub>x</sub> (SO<sub>2</sub> + SO<sub>4</sub>) and NO<sub>x</sub> (NO + NO<sub>2</sub>) and refer the reader to Table 1 where the CCP emissions of NO<sub>x</sub> are documented. It is noted that NO<sub>2</sub> emissions are present and make up about 3% of the NO<sub>x</sub> on a molar basis. However, the use of a caustic solution in the CCP would reduce concentrations of NO<sub>2</sub> in the flue-gas to trace amounts. Can the authors provide justification of why this was not considered when modelling the emissions of NO<sub>x</sub> from the CCP?**

**Response:**

NO<sub>2</sub> typically constitutes 5% v/v of NO<sub>x</sub> after flue gas treatment. In the very basic solution (the solution is caustic because NaOH is added to reclaim some of the MEA) in the absorber column, MEA reacts selectively with NO<sub>2</sub> causing oxidative degradation of the amine. However, we do not agree with the referee's statement, that NO<sub>2</sub> would be reduced to trace amounts after the CCP. In fact, the removal of total NO<sub>x</sub> in the CO<sub>2</sub> capture process is found to be very small, reported values are 0.8% (Knudsen et al., 2006) and 1.25% (Rao and Rubin, 2002). Using the higher reported NO<sub>x</sub> reduction of 1.25% and assuming that only NO<sub>2</sub> is removed, the removal of NO<sub>2</sub> in the CO<sub>2</sub> capture process is estimated to be 25%. This NO<sub>2</sub> removal percentage is in agreement with the value used in the study by Koorneef et al. (2008). Rao and Rubin (2002) give a range of 20-30% NO<sub>2</sub> removal. To give another example, the environmental impact assessment study by Veltman et al. (2010), estimated that a 420 MW gas-fired power plant equipped with CCP using MEA-based capture (designed for the capture of 1.3x10<sup>6</sup> tonnes CO<sub>2</sub> per year) emits 2.9x10<sup>4</sup> kg NO<sub>2</sub> per year to air, based on 25% NO<sub>2</sub>-removal. Their CCP NO<sub>2</sub> emissions correspond to 0.92 g/s, four times higher than the applied NO<sub>2</sub> emission in our study (0.22 g/s; Table 1). The year-to-year variability of NO<sub>x</sub> emissions from the power plant in Mongstad is high (~35%) with a range of 90-190 tonnes NO<sub>x</sub> per year (we use the central estimate of 140 tonnes NO<sub>x</sub> per year). Given the large year-to-year variability of the NO<sub>x</sub> emission factor and the uncertainty of the NO<sub>2</sub> mixing ratio in the treated flue gas, we neglected the effect of selective NO<sub>2</sub> removal on the emissions of NO<sub>2</sub> from the fictive CCP.

- 5. *There is some focus on the sensitivity of peak MEA+DEYA concentrations in the model cell which contains the CCP facility. In discussing this sensitivity the authors should also note that the peak concentrations will be a function of the cell volume and may be the subject of errors due overshoot/undershoot of the numerical advection scheme which is not able to accurately resolve single cell emissions close to the point of emission. In fact, given the small sensitivity of the primary emissions to chemistry close to the stack, did the authors give consideration to using a Gaussian plume or similar model for resolving the near-field concentrations?***

**Response:**

The point source emission is assumed to immediately mix within the volume of the model grid-box (here 2000 x 2000 x 90 m<sup>3</sup> in the inner domain), whereas a typical point-source plume does not expand to the size of the grid cell for a substantial time period, depending on the meteorological situation. In the case of NO emissions from the point source, instantaneous

mixing will cause higher rates of titration of background O<sub>3</sub> by emitted NO in the grid cell. Consequently, O<sub>3</sub> ground concentrations in the vicinity of the source will be lower in the Eulerian model compared to a reactive plume model. However, by comparing modelled O<sub>3</sub> ground concentration to measured O<sub>3</sub> concentration at Hamna (located 3 km downwind the source) we can show that daily average concentrations are in good agreement throughout January to September 2007 (Figure 5). Based on this no indications of overshoot/undershoot were found.

We have previously performed a model study to assess the impact of amine emissions from a large scale CCP (Karl et al., 2011) using TAPM (“The Air Pollution Model”) which has a built-in sub-grid Lagrangian particle dispersion model to resolve dispersion of a point source plume. The results from the comparison with TAPM are shown in section 3.7 and in the Supplement, demonstrating similar dispersion of the plume on the yearly average. We noted a good agreement of the maximum monthly mean air concentration of an inert tracer at the ground level. Amine concentrations close to the point source computed by WRF-EMEP and TAPM were in a range of 20 – 140 ng m<sup>-3</sup> and 30 – 140 ng m<sup>-3</sup>, respectively (section 3.7 in the manuscript, Table S7 in the Supplement). The TAPM simulation had a wider impact area with concentrations > 10 ng m<sup>-3</sup> and a lower maximum (30 ng m<sup>-3</sup> instead of 45 ng m<sup>-3</sup>), see Figure S9 in the Supplement.

The reason for the wider dispersion might be the advection from a point source with grid-cell size. However, as shown with the Gaussian plume sensitivity test in the reply to Point 2 of the referee, different plume rise parameterization in the two models and more frequent occurrence of moderately stable cases in the TAPM simulation (which uses different meteorological data) could be plausible explanations for the wider impact area.

We added a comparison for July 2007 (Figure C3), showing similar dispersion pattern in both models.

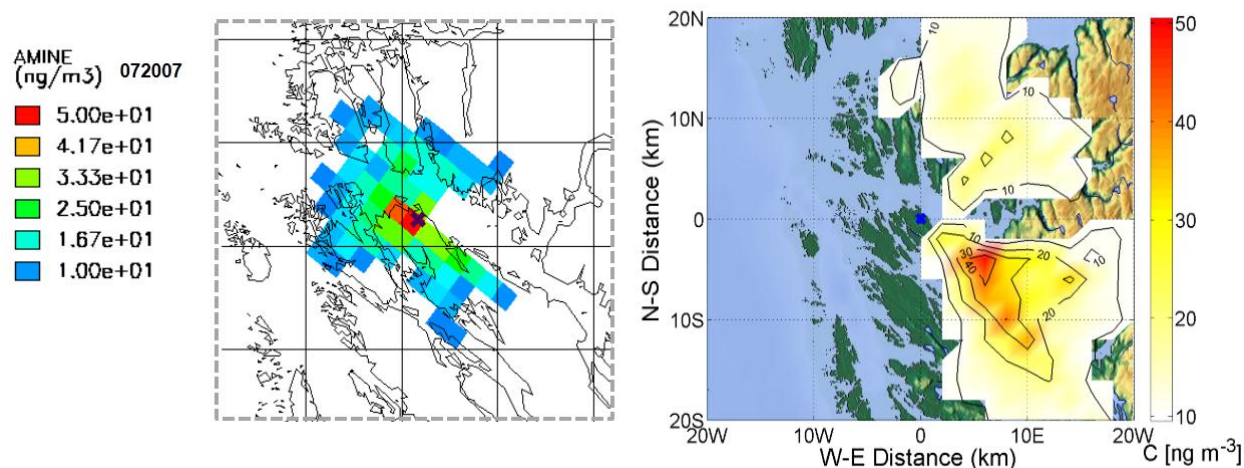


Figure C3: Comparison of the July 2007 average ground-level air concentration of a chemically inert tracer (in ng m<sup>-3</sup>) emitted from the CCP with unity emission rate (1 g s<sup>-1</sup>). Left side in the WRF-EMEP simulation (reference scenario) and right side in the TAPM simulation of the worst case scenario study by Karl et al. (2011).

For better visibility of the comparison that we did for amine concentrations with the TAPM model, the Supplement figure S9 will be moved into the main manuscript text, section 3.7, as new Figure 10. The comparison for July 2007 (Figure C3) will be added as well.

The following note was added to the text in section 3.7 (“Comparison with TAPM simulation results”) on page 8661, line 6:

“The reason for the (on yearly average) narrower dispersion in the EMEP model might be the advection from a point source with grid-cell size ( $2 \times 2 \text{ km}^2$ ). However, different plume rise parameterization in the two models and more frequent occurrence of moderately stable cases in the TAPM simulation (which uses different meteorological data) are also plausible explanations for different maximum concentrations and different extents of the impact area.”

**6. *In nesting from 50 km to 2 km, the model grid spacing decreased by a factor 5 for each grid nest. A more typical reduction is a factor of 3 in order to minimise aliasing errors. How do the authors justify the larger factor?***

**Response:**

The referee is probably right that a nest factor of 3 is more commonly used than 5. Although the nest factor 3 is most tested, it is acceptable to use a nesting ratio of 5 in WRF-ARW. In fact, both 3 and 5 are “recommended nest factors” according to the WRF model user guide (see e.g. the latest WRF tutorials given here:

[http://www2.mmm.ucar.edu/wrf/users/tutorial/tutorial\\_presentation\\_winter\\_2014.htm](http://www2.mmm.ucar.edu/wrf/users/tutorial/tutorial_presentation_winter_2014.htm)).

Furthermore, our use of the WRF-EMEP results are only from the inner part ( $40 \times 40 \text{ km}^2$  zoom region) of the inner domain ( $200 \times 200 \text{ km}^2$ ) with a long distance (in terms of grid cells) from the domain boundaries. Thus any uncertainties caused by the large nest factor (due to the transition from a coarser resolution to a nested finer resolution) will be minimized. Furthermore, we are merely interested into the dispersion of a tracer released from a single point source and not into the transport of a tracer from outside into the region (e.g. by long-range transport). We have shown in the manuscript (section 3.5) that the contribution related to the recirculation of MEA from the coarser (10-km resolution) outer domain to the MEA-budget in the inner domain is very small (less than 2% of the emitted amount). Finally, our choice of a nest factor of 5 was based on the aforementioned facts and, of course, that the factor of 5 is cheaper CPU-wise than a factor of 3. The latter consideration was an important point, since the model system was CPU-demanding.

**7. *In section 3.2 the authors provide a comparison of NO, NO<sub>x</sub>, O<sub>3</sub> and O<sub>x</sub>. Note that contemporary observations of NO<sub>2</sub> and actually the sum of NO<sub>2</sub> + HNO<sub>3</sub> + PAN etc. and thus the modelled ‘NO<sub>2</sub>’ should consist of the same summation. This is particularly important for aged air masses. Can the authors confirm that the comparison of observed and modelled ‘NO<sub>2</sub>’ was done this way?***

**Response:**

Measurements were done in a distance of ca. 3 km downwind the source. Mongstad refinery is the highest emitter of NO<sub>x</sub> within a radius of 40 km or more. Mongstad receives for most of the time clean marine air masses from the Atlantic. HNO<sub>3</sub> and PAN are expected to have a small



contribution (to the sum  $\text{NO}_2 + \text{HNO}_3 + \text{PAN}$ ) since they are commonly connected to aged air masses. Model simulations for July 2007 show that daily mean ground-level air concentrations at Hamna are in the range of 0.23 – 3.73 ppbv  $\text{NO}_2$ , 0.081 – 0.55 ppbv PAN and 0.015 – 0.57 ppbv  $\text{HNO}_3$ , respectively. Modelled concentrations of PAN +  $\text{HNO}_3$  are about a factor of 3-4 lower than the corresponding modelled concentrations of  $\text{NO}_2$ . For the measurement of NO and  $\text{NO}_2$  at Hamna, the API T200 ([http://www.teledyne-api.com/manuals/06858D\\_T200.pdf](http://www.teledyne-api.com/manuals/06858D_T200.pdf)) was used. The Model T200 Nitrogen Oxides Analyzer uses chemiluminescence detection for ambient monitoring of nitric oxide (NO), nitrogen dioxide ( $\text{NO}_2$ ) and the total nitrogen oxides ( $\text{NO}_x$ ).  $\text{NO}_2$  is reduced to NO with the catalytic converter (molybdenum, Mo). By converting the  $\text{NO}_2$  in the sample gas into NO, the analyser can measure the total  $\text{NO}_x$  content of the sample gas (i.e. the NO present + the converted  $\text{NO}_2$  present). The T200 includes a special  $\text{HNO}_3$  desorber which eliminates any  $\text{HNO}_3$  before it can be converted into NO by the analyser's converter. For the above mentioned reasons, we did not use the summation of modelled  $\text{NO}_2 + \text{HNO}_3 + \text{PAN}$  for the comparison with measured  $\text{NO}_2$ .

## References:

Holtslag, A., E. De Bruijn, and H.L. Pan, 1990: A High Resolution Air Mass Transformation Model for Short-Range Weather Forecasting. *Mon. Wea. Rev.*, 118, 1561-1575.

Karl, M., Wright, R. F., Berglen, T. F., and Denby, B.: Worst case scenario study to assess the environmental impact of amine emissions from a  $\text{CO}_2$  capture plant, *Int. J. Greenh. Gas Con.*, 5, 439-447, 2011.

Koorneef, J., van Keulen, T., Faaij, A., and Turkenburg, W., Life cycle assessment of a pulverized coal power plant with post-combustion capture, transport and storage of  $\text{CO}_2$ , *Int. J. Greenh. Gas Con.*, 2, 448-467, 2008.

Knudsen, J. N., Vilhelmsen, P.-J., Biede, O., and Jensen, J. N.: CASTOR 1 t/h  $\text{CO}_2$  absorption pilot plant at the Elsam Kraft A/S Esbjerg power plant—First year operation experience, In: *Proceedings of the Greenhouse Gas Control Technologies*, vol. 8, Trondheim, Norway, 2006.

Rao, A. B. and Rubin, E. S.: A technical, economic, and environmental assessment of amine<sub>30</sub> based  $\text{CO}_2$  capture technology for power plant greenhouse gas control, *Environ. Sci. Technol.*, 36, 4467–4475, 2002.

Slørdal, L. H., Solberg, S., and Walker, S. E.: The Urban Air Dispersion Model EPISODE applied in AirQUIS2003. Technical description. Norwegian Institute for Air Research, Kjeller, NILU TR 12/03, 2003.

Veltman, K., Singh, B., and Hertwich, E. G.: Human and environmental impact assessment of postcombustion  $\text{CO}_2$  capture focusing on emissions from amine-based scrubbing solvents to air, *Environ. Sci. Technol.*, 44, 1496-1502, 2010.

Walker S. E., Slørdal L. H., Guerreiro C., Gram F., and Grønskei, K. E.: Air Pollution exposure monitoring and estimation. Part II. Model evaluation and population exposure. *J. Environ. Monit.*, 1, 321-326, 1999.